Oxidative Metamorphosis of Poly(Styrenedisulfide) Backbone

R. Latha,* K. Ganesh, and K. Kishore

Department of Inorganic and Physical Chemistry, Indian Institute of Science, Bangalore-560 012, India

Received November 5, 1998; Revised Manuscript Received November 12, 1999

ABSTRACT: This is the first report on the oxidation of a disulfide polymer, viz., poly(styrenedisulfide) (PSD). Oxidation was performed using $KMnO_4$ and $KHSO_4$, which are strong and mild oxidizing agents, respectively. Fourier transform−infrared spectroscopy (FT−IR) and intrinsic viscosity ([η]) measurements revealed that degradation of PSD occurs to some extent during oxidation when $KMnO_4$ was used. Further, FT−IR and [η] results indicated that the oxidation of PSD using $KMnO_4$ is better in heterogeneous conditions than under phase-transfer medium because the degradation was curtailed in the former case. Direct pyrolysis−mass spectrometry (DP−MS), Fast atom bombardment mass spectrometry (FABMS) and pyrolysis−gas chromatography−mass spectrometry (Py−GC−MS) analyses of the oxidized PSD was carried out and the obtained results corroborate well with the FT−IR and [η] studies. Increased rigidity of the oxidized polymers which is reflected in their T_g and [η] values, compared to PSD, was further confirmed by the radius of gyration (R_g) and trans percentage data calculated from the molecular dynamics simulations studies.

Introduction

Polymer-to-polymer transformations are of great importance because new polymers could be made in those cases where the required monomer does not exist or the monomer does not polymerize (or polymerizes with difficulty).[1,2] Polymer transformations could be broadly classified as backbone transformation and side chain transformation. In general, the side chain modifications such as ester hydrolysis, esterification, etherification, sulfonation, halogenation, and oxidation are well studied.[1,3,4] Oxidative metamorphosis of polymer backbone has not been much studied except for reports on the oxidation of some polymonosulfides.[3−18] We wish to examine here successive oxidative metamorphosis of a disulfide polymer backbone to its respective mono-, di-, tri- and tetraoxide counterparts. Such backbone modifications on sulfide polymers is of considerable technological importance because the resultant oxidized polymers may find wide applications as oxidizing agents, compatibilizers, polymeric solvents, insulating materials, biocompatible membranes, etc.[8,10]

Our main aim here is to examine as to how the flexibility of the polymer varies during such oxidative backbone transformations. Such investigations have not been carried out hitherto on disulfide polymers. We have chosen poly(styrenedisulfide) (PSD) in the present study where considerable studies including its flexibility have been reported recently from our laboratory.[19−24,28] The final product of the backbone oxidative transformation of PSD is poly(styrenedisulfone) (PSDS). It may be pointed out that direct synthesis of PSDS through a monomer route is not possible and hence backbone metamorphosis remains the only choice for preparing PSDS and polydisulfones in general. In the present study, we have chosen a strong oxidizing agent[29−31] ($KMnO_4$) and a mild oxidizing agent[32] ($KHSO_4$) to bring about the backbone oxidation of PSD.

Experimental Section

Materials. PSD was synthesized from styrene dibromide and Na_2S_2 as described elsewhere.[24] Chloroform, methanol, tetrahydrofuran, and dimethyl sulfoxide were purified by distillation before use. Dichloromethane was purified as reported earlier.[29] Analar grade $KMnO_4$, $KHSO_4$, $CuSO_4{\cdot}5H_2O$, tetra-*n*-butylammonium bromide (TBAB), and anhydrous Na_2SO_4 were used as such.

Typical Procedure for the Oxidation of PSD. Oxidation under Phase-Transfer Conditions. Oxidation of PSD (1 mol equiv in $CHCl_3$) was performed either by taking different mole equivalents of the oxidant ($KMnO_4$ or $KHSO_4$ = 1, 2, or 4 mol equiv) for a constant reaction time of 6 h or by varying the reaction time (2, 6, 12, or 24 h) for a constant oxidant concentration (1 mol equiv). An aqueous solution of the oxidant was added to a $CHCl_3$ solution of PSD in the presence of the phase-transfer catalyst, TBAB. The reaction mixture was stirred at room temperature for the required time. The $CHCl_3$ layer from the reaction mixture was separated, washed several times with water, and dried over anhydrous Na_2SO_4. The $CHCl_3$ solution was concentrated by rotary evaporation, and adding excess methanol precipitated the oxidized polymer. The polymer was dried under vacuum for a constant weight.

Oxidation under Heterogeneous Conditions. Oxidation of PSD in CH_2Cl_2 using 1, 2, or 4 mol equiv of $KMnO_4$ was carried out under heterogeneous conditions in the presence of $CuSO_4{\cdot}5H_2O$ as reported elsewhere.[29] The reaction mixture was stirred under reflux for 6 h, cooled to room temperature, and filtered through a sintered glass funnel. Adding excess methanol, after concentrating the CH_2Cl_2 solution by rotary evaporation, precipitated the oxidized polymer. The polymer was vacuum-dried to a constant weight.

Measurements. Fourier transform−infrared (FT−IR) spectra of the neat polymer films were recorded on a Brucker IFS-55 spectrometer. A fast atom bombardment mass spectrometric (FABMS) study was done on a JEOL SX 102/DA-6000 mass spectrometer using xenon (6KV, 10 mA) as the FAB gas. The accelerating voltage was 10 kV, and the spectrum was recorded at room temperature in the positive mode. Thioglycerol was used as the matrix; the matrix peaks appear at *m*/*z* 91, 109, 217. A direct pyrolysis−mass spectrometric (DP−MS) analysis was done using both electron impact (EI) at 18 eV and chemical ionization (CI) in the positive mode using methane as the reagent gas.[24,28]

For pyrolysis GC−MS (Py−GC−MS) studies, the sample was placed in a Curie point metal sleeve and pyrolyzed at 740 °C for 0.3 s in the JHP-35 pyrolysis unit. The volatiles were swept through the needle interface at 250 °C and then onto

10.1021/ma981715d CCC: $19.00 © 2000 American Chemical Society
Published on Web 04/13/2000

Scheme 1

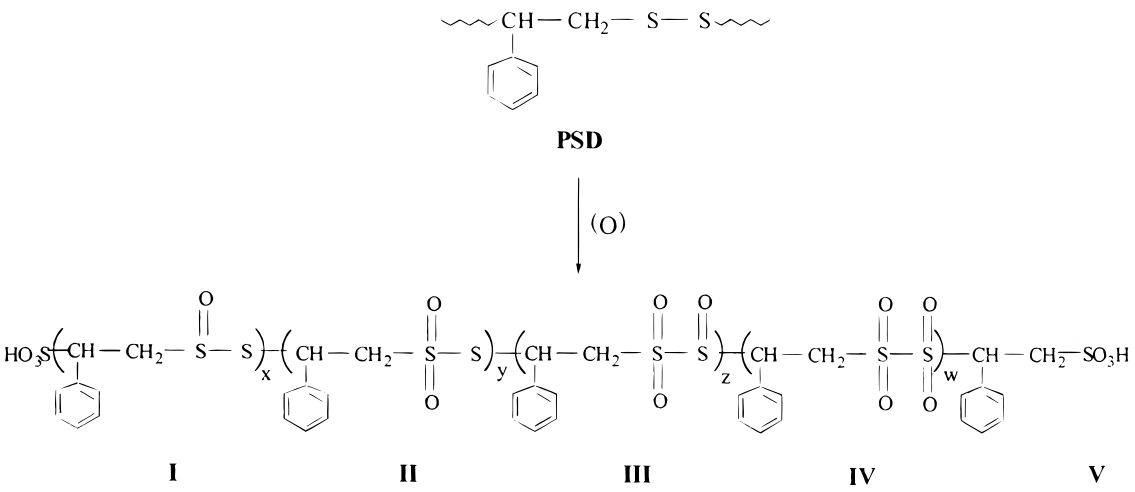

the analytical column. The column was heated from 0 to 325 °C (10 min hold) at 10 °C/min. The separated components were subjected to electron bombardment at 70 eV. A full scan unit resolution mass spectrum from *m*/*z* 29 to *m*/*z* 600 was recorded.

For elemental analysis, the oxidized samples were first subjected to acid digestion. Approximately 0.6 g of sample in duplicate was placed into a fluoropolymer container with 5 mL of nitric acid and 1 mL of hydrogen peroxide. The vessels were sealed and placed into the microwave oven for digestions. The final digestates were diluted with DI water in 200 mL volumetric flasks. The samples were analyzed for sulfur using a calibrated Thermo Jarrell Ash 61E inductively coupled plasma optical emission spectrometer.

Differential scanning calorimetric (DSC) measurements of the polymers (10−14 mg) were carried out in nitrogen atmosphere using a Perkin-Elmer 7 series thermal analysis system. The glass transition temperature (T_g) of all samples was obtained at a heating rate of 2 °C/min.

Intrinsic viscosity [η] measurements were done on a Schott−Gerate viscometer using THF or DMSO as the solvent at 25 °C.

Results and Discussion

Oxidation of PSD was performed using two different oxidizing agents: $KMnO_4$ and $KHSO_4$. $KMnO_4$ oxidation was carried out in a phase-transfer medium ($CHCl_3$/H_2O) as well as under heterogeneous conditions (CH_2Cl_2), while $KHSO_4$ oxidation was done only by phase-transfer method.

FT−IR. It is well-known that the oxidation of simple disulfides[6,7] proceeds in a stepwise manner to give thiosulfinate (**I**), thiosulfonate (**II**), sulfonylsulfoxide (**III**), disulfone (**IV**) and finally sulfonic acid (**V**) (Scheme 1).

Because of the polymeric nature of PSD, unlike simple disulfides, the oxidation produces a random copolymer that contains all the groups (Scheme 1), and the concentration of each of these groups depends on various factors such as the nature of the oxidant, time of oxidation and oxidant concentration, etc. Ascertaining and quantifying these groups (**I**−**IV**) individually by FT−IR is arduous owing to the marginal difference in their S═O stretching frequencies. Since the $\nu_{S=O}$ is different for the groups SO and SO_2, they are followed to calculate the extent of oxidation. A typical FT−IR spectrum of the oxidized PSD is given in Figure 1. IR absorption around 3000, 1450, and 1490 cm^{-1} showed the presence of a phenyl group with overtones from 1600 to 2000 cm^{-1}. The strong bands at 690 and 750 cm^{-1} revealed that the phenyl group is monosubstituted. The

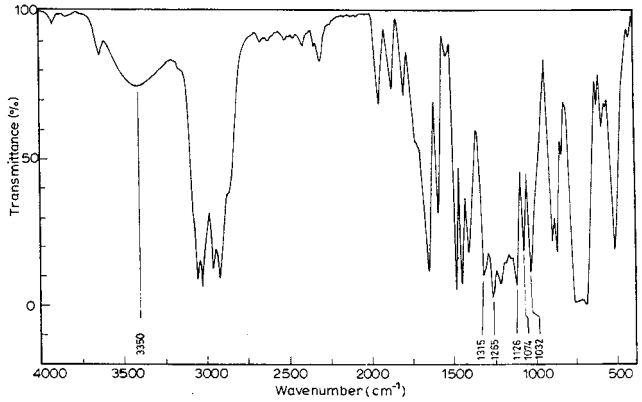

Figure 1. FT−IR spectrum of oxidized PSD ($KMnO_4$ phase-transfer oxidation, 1 mol equiv, reaction time 6 h).

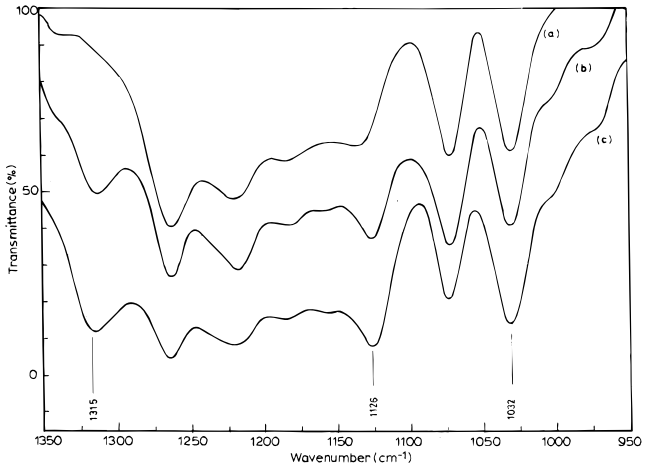

Figure 2. FT−IR spectra of three $KMnO_4$ phase-transfer oxidized samples: (a) 1 mol equiv of oxidant; (b) 2 mol equiv; (c) 4 mol equiv. Reaction time: 6 h.

broad absorption around 3350 cm^{-1} indicated the presence of the $-SO_3H$ group, which is evidence for the degradation of PSD during oxidation. The bands at 1126 and 1315 cm^{-1} showed the presence of a SO_2 group, while the absorption at 1032 cm^{-1} confirmed the presence of SO. The extent of oxidation was calculated from the ratio of the optical densities (A_{SO}/A_{SO_2}) of $\nu_{S=O}$ stretching bands of SO and SO_2 groups occurring at 1032 and 1126 cm^{-1} respectively (Figure 2). Figure 3 shows A_{SO}/A_{SO_2} as a function of the concentration of the oxidant. For $KMnO_4$ oxidation, the ratio A_{SO}/A_{SO_2} de-

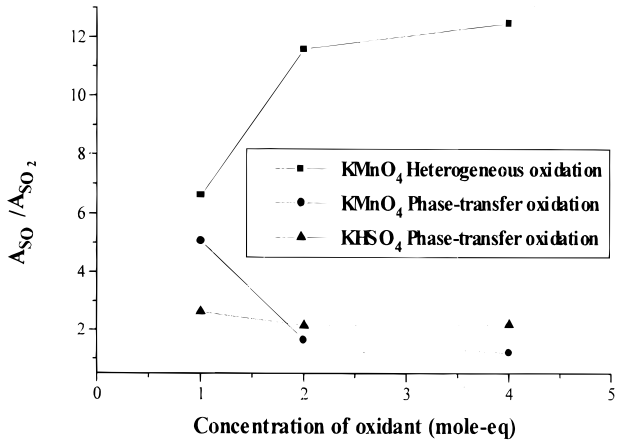

Figure 3. Extent of oxidation as a function of oxidant concentration. Reaction time: 6 h.

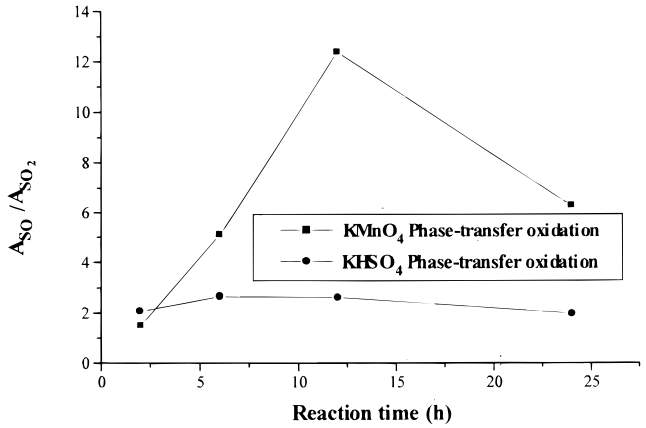

Figure 4. Extent of oxidation as a function of reaction time. Oxidant concentration was 1 mol equiv.

creases as the oxidant concentration increases under phase-transfer conditions. On the contrary, in $KMnO_4$-heterogeneous oxidation the ratio A_{SO}/A_{SO_2} increases. This implies that the concentration of SO increases in the heterogeneous oxidation and that of SO_2 increases in the phase-transfer oxidation as the oxidant concentration increases. It is reported earlier that oxidation of methylphenyl sulfide using permanganate under heterogeneous medium could not proceed to completion due to the precipitation of MnO_2 on the surface of the oxidant.[33] Most probably, due to the same reason, here also the heterogeneous oxidation proceeds largely to thiosulfinate. The ratio A_{SO}/A_{SO_2} does not decrease much as the concentration of $KHSO_4$ was increased since it is a mild oxidizing agent in comparison with $KMnO_4$ (Figure 3).

To study the effect of the reaction time on the extent of oxidation, the ratio A_{SO}/A_{SO_2} was plotted against reaction time for $KMnO_4$ and $KHSO_4$ (Figure 4). In both $KMnO_4$ and $KHSO_4$ oxidation, the ratio A_{SO}/A_{SO_2} first increases and then decreases, which implies that initially more SO is formed and as the time elapses the SO_2 concentration increases. However, in $KHSO_4$ oxidation the extent of oxidation was far less since $KHSO_4$ is a milder oxidizing agent than $KMnO_4$.

Elemental Analysis. Table 1 displays the elemental analysis data of the oxidized PSD samples. The experimentally determined sulfur percentage of the oxidized polymers revealed that the average structure is between poly(styrenethiosulfinate) and poly(styrenesulfonylsulfoxide). It is to be noted here that the average structure

Table 1. Elemental Analysis Data of Oxidized Polymers

Structure of PSD and its various oxidized counterparts	Theoretical Sulfur Percentage	Oxidized Samples	Experimental Sulfur Percentage
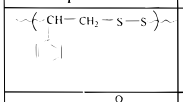	38.09	KM1-24	31.5
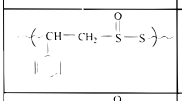	34.78	KM2-6	32.8
		KM4-6	31.9
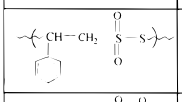	32.00	KMH2-6	31.2
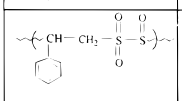	29.63	KMH4-6	30.3
		KH1-24	33.5
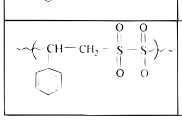	27.59	KH4-6	33.3

*KM1−24, KM2−6, KM4−6: $KMnO_4$ phase-transfer oxidized samples (1−24, 1 mol equiv, 24 h; 2−6, 2 mol equiv, 6 h; 4−6, 4 mol equiv, 6 h). KMH2−6, KMH4−6: $KMnO_4$ heterogeneous oxidized samples (2−6, 2 mol equiv, 6 h; 4−6, 4 mol equiv, 6 h). KH1−24, KH4−6: $KHSO_4$ phase-transfer oxidized samples (1−24, 1 mol equiv, 24 h; 4−6 mol equiv, 6 h).

refers to a statistical mean of all possible oxidized structures. Similar to the FT−IR results, for both $KHSO_4$- and $KMnO_4$-oxidized samples, the percentage of oxidation increases with the oxidant concentration, which is reflected in the decrease of sulfur percentage. Besides, it also corroborates the FT−IR observation that $KHSO_4$ is a milder oxidizing agent compared to $KMnO_4$.

Mass Spectrometry. Determination of primary degradation products by the DP−MS technique[25−27] and the primary degradation products of PSD has been reported elsewhere.[24,28] The DP−MS (EI and CI) and the respective primary degradation products of the oxidized PSD are displayed in Figure 5 and Table 2, respectively. The FABMS of oxidized PSD is also shown in Figure 5. The structures referring to individual FABMS peaks are included as well in Table 2. It is difficult to characterize the peaks beyond *m/z* 152 in the EI, CI, and FABMS due to both the isoelectronic nature of S and O_2 and the random placement of SO and SO_2 groups along the PSD backbone (see Scheme 1). The detection of styrene (*m/z* 105, MH^+) and 1-phenylethanesulfonic acid (*m/z* 186) in the FABMS (Figure 5 and Table 2) clearly indicates that PSD undergoes degradation during oxidation, which supports the FT−IR results discussed earlier.

The thermal degradation of poly(styrenesulfone) is reported to yield styrene and SO_2 as the major products.[34] In the present case, since both S_2 and SO_2 have the same *m/z* value (64), it is very difficult to differentiate them in the EI mass spectrum (Figure 5). To overcome this difficulty, Py−GC−MS analysis has been carried out for three different oxidized samples of PSD (Figure 6). The Py−GC−MS products identified are CO_2, H_2S, COS, SO_2, CS_2, ethylbenzene, styrene, phenylethene-1-thiol, benzothiophene, 2,3-dihydrobenzothiophene, and diphenylthiophene (Table 3). It is to be noted here that neat PSD under Py−GC−MS conditions produces large amounts of S_2 including other products.[28] Since S_2 is absent in the Py−GC of oxidized PSD, it is inferred that the presence of unoxidized disulfide linkages are negligible and the *m/z* 64 peak in the EI spectrum (Figure 5) of oxidized PSD is due to SO_2 and

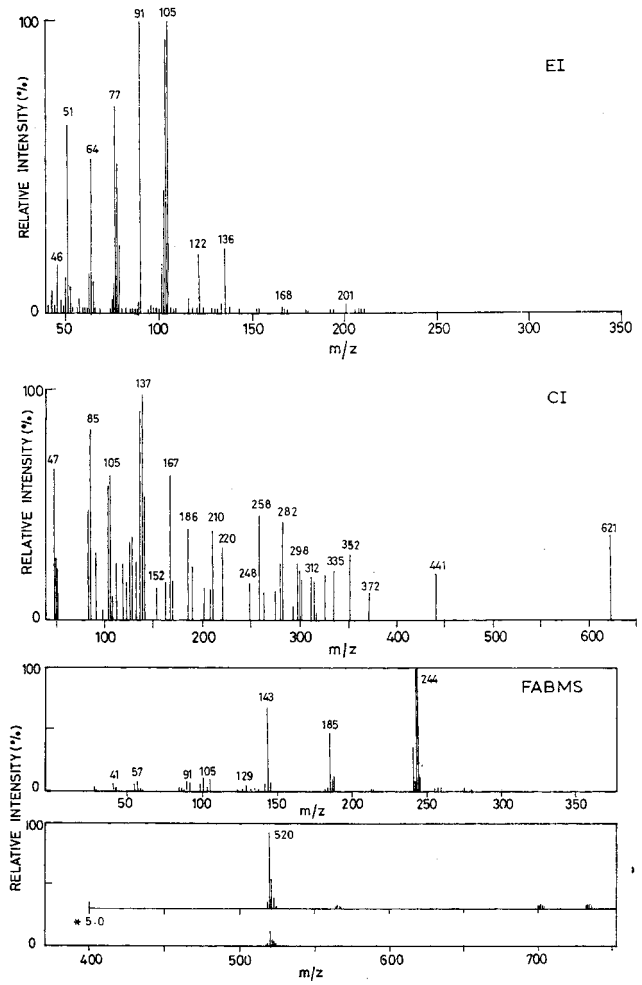

Figure 5. Mass spectra of oxidized PSD ($KMnO_4$ phase-transfer oxidation, 1 mol equiv, reaction time 6 h).

not S_2. The Py−GC−MS traces of the oxidized PSD samples show that the intensity of the SO_2 signal increases as the concentration of $KMnO_4$ increases (signal 4, Figure 6b,c), which is in accordance with the FT−IR results discussed earlier (Figure 3).

Intrinsic Viscosity [η]. Intrinsic viscosities of all the $KMnO_4$ oxidized polymers in THF were less compared to that of the parent polymer, viz., PSD (Figures 7 and 8). A decrease in [η] of the oxidized polymer indicates that PSD undergoes degradation during oxidation which is corroborated by the FT−IR and FABMS studies. It is to be noted here that a similar behavior has also been observed during the oxidation of monosulfide polymers.[5]

Effect of Solvent. To study the effect of solvent on the oxidized polymer, [η] was also measured in DMSO (Figure 7 and 8). DMSO is a good solvent for the oxidized PSD as there are favorable dipole−dipole interactions between the S═O bonds of the solvent and that of the oxidized polymer. Hence, in DMSO, the oxidized PSD will be in an extended conformation as a result its hydrodynamic volume will be more, that is why [η] of the oxidized PSD was higher in DMSO than in THF (Figures 7 and 8).

Effect of Reaction Time. Figure 7 shows the plot of [η] as a function of reaction time for 1 mol equiv concentration of the oxidant. For $KMnO_4$ phase-transfer oxidation, the rate of decrease of [η] was initially greater, followed by a gradual decrease indicating random cleavage of the backbone. However, in the case

Table 2. Molecular Ions of the Products Detected in the DP−MS and FABMS of Oxidized PSD

Structure	M^+ in EI (m/z)	MH^+ in CI (m/z)	FABMS (m/z)
CH_2S	46	47	
S_2 or SO_2	64*		
	104	105	105 (MH^+)
	122	123	
	136	137	
	153 (MH^+)	153	
	168*	168* (M^+)	
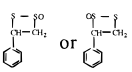			185* (MH^+)
		186 (M^+)	186 (M^+)
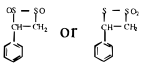	201* (MH^+)	201*	
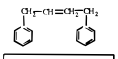	208	208 (M^+)	
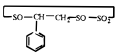		263*	
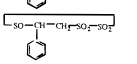		281*	
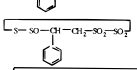		312*	
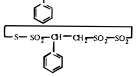		327*	

*Difficult to assign structures for these *m/z* values because S and O_2 are isoelectronic and SO and SO_2 are placed randomly during oxidation.

of $KHSO_4$ oxidation, the [η] initially decreases and then increases. Furthermore, the rate of initial decrease of [η] in $KHSO_4$ oxidation is not as high as observed in $KMnO_4$ oxidation, the reason being as follows.

The lower rate of initial decrease of [η] in $KHSO_4$ oxidation than in $KMnO_4$ oxidation is because $KHSO_4$ is relatively a mild oxidizing agent. In $KMnO_4$ oxidation, the reduction of MnO_4^- to MnO_2 in an aqueous medium liberates hydroxyl ions, and the reaction mixture becomes alkaline as the oxidation proceeds.[31,33] Hence, when the oxidation is performed under phase-transfer conditions it is most likely that the base generated from $KMnO_4$ may also trigger the degradation of the polymer, thereby reducing its molecular weight to a considerable extent which is reflected in the [η]. Also, there is no base formation in $KHSO_4$ oxidation that might trigger the degradation of the polymer chain as is observed in the case of $KMnO_4$.

Effect of Concentration of Oxidant. Figure 8 shows the plot of [η] as a function of oxidant concentration. For $KMnO_4$ phase-transfer oxidation, the [η] initially decreases from 1 to 2 mol equiv due to degradation but subsequently increases from 2 to 4 mol equiv of oxidant. However, when the oxidation was performed under heterogeneous conditions there was negligible variation in the [η] values. Under heterogeneous conditions, the mechanism of oxidation being different,[29] the base hydrolysis, which also triggers degradation, is minimized. Because of this, the considerable initial reduction in [η] which was observed in the case of $KMnO_4$ phase-transfer oxidation is not encountered

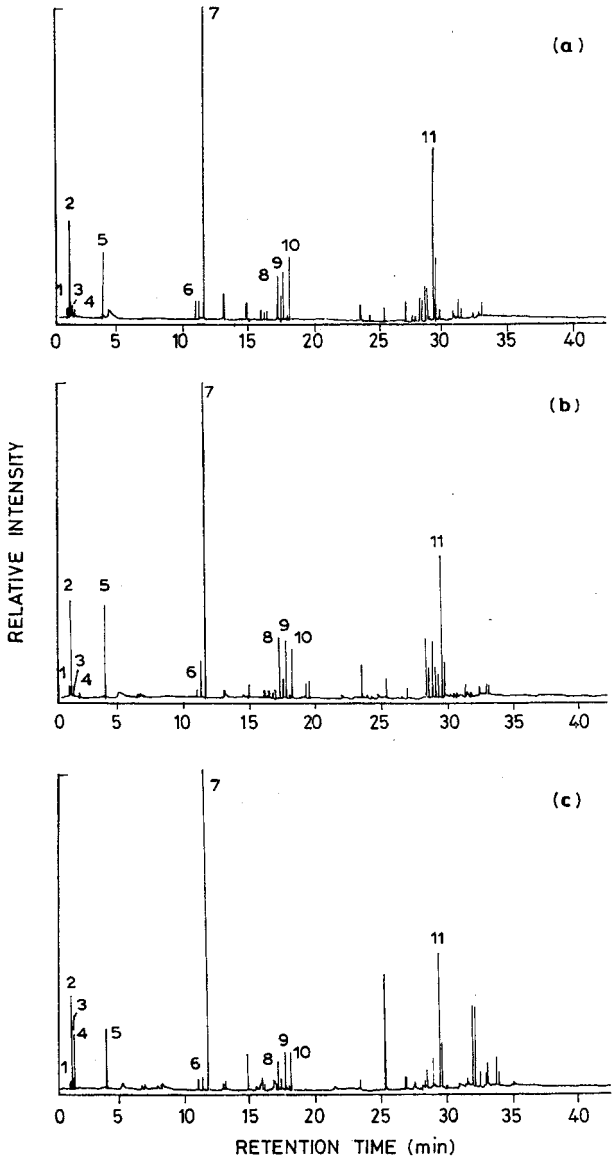

Figure 6. Py−GC−MS pyrograms of three oxidized PSD samples: (a) $KHSO_4$ phase-transfer oxidation (1 mol equiv, reaction time 6 h); (b and c) $KMnO_4$ phase-transfer oxidation (1 mol equiv, reaction time 6 h, and 4 mol equiv, reaction time 6 h, respectively).

here. In $KHSO_4$ phase-transfer oxidation, the oxidized PSD has higher [η] than neat PSD and there is an increase in the [η] of all of the oxidized polymers compared to neat PSD. In $KMnO_4$ phase-transfer oxidation too, the [η] shows an increase when 2−4 mol equiv of oxidant was taken. Such an increase in [η] values during backbone oxidation of a polymer is rather unusual because one would always expect [η] to go down on account of the breakage of the polymer backbone. The only way it could be explained is by considering the conformational changes that might occur during the oxidation of the polymer backbone. Introduction of a SO_2 group restricts bond rotation because of electrostatic interactions between the dipoles ($\overrightarrow{S{=}O}$), which locks the conformation that decreases flexibility, and hence the chain becomes stiff.[35] As more and more of the SO_2 groups are incorporated during oxidation, it enhances the stiffness of the polymer backbone which may lead to higher hydrodynamic volumes resulting in an increase of [η] values. Increases in the chain stiffness

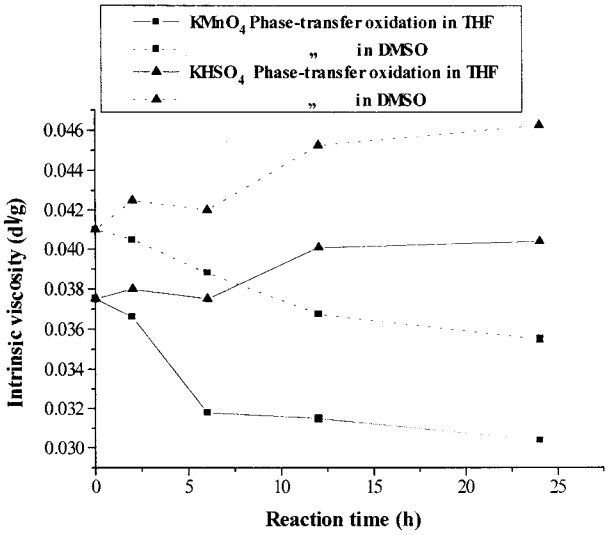

Figure 7. Intrinsic viscosity as a function of reaction time in different solvents. Oxidant concentration was maintained at 1 mol equiv.

Table 3. Assignments of the Peaks Corresponding to Pyrolysis Compounds Obtained in the Py−GC−MS of Three Different Oxidized Polymers

Peak label	m/z	Compound
1	44	CO_2
2	34	H_2S
3	60	COS
4	64	SO_2
5	76	CS_2
6	106	
7	104	
8	134	
9	136	
10	136	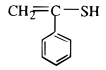
11	236	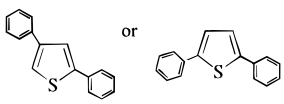

when sulfide linkages in a polymer are oxidized to sulfone are reported in the literature.[9] This was further confirmed from the glass transition data; the T_g values of the oxidized PSD were found to be higher than that of the neat PSD (Table 4), confirming the fact that the oxidized PSD is more rigid compared to neat PSD.

Molecular Dynamics. To examine how the flexibility changes with successive oxidation of disulfide linkages of PSD backbone, molecular dynamics (MD) simulation studies have been performed for PSD and all the possible structures of oxidized PSD (Scheme 2).

Scheme 2

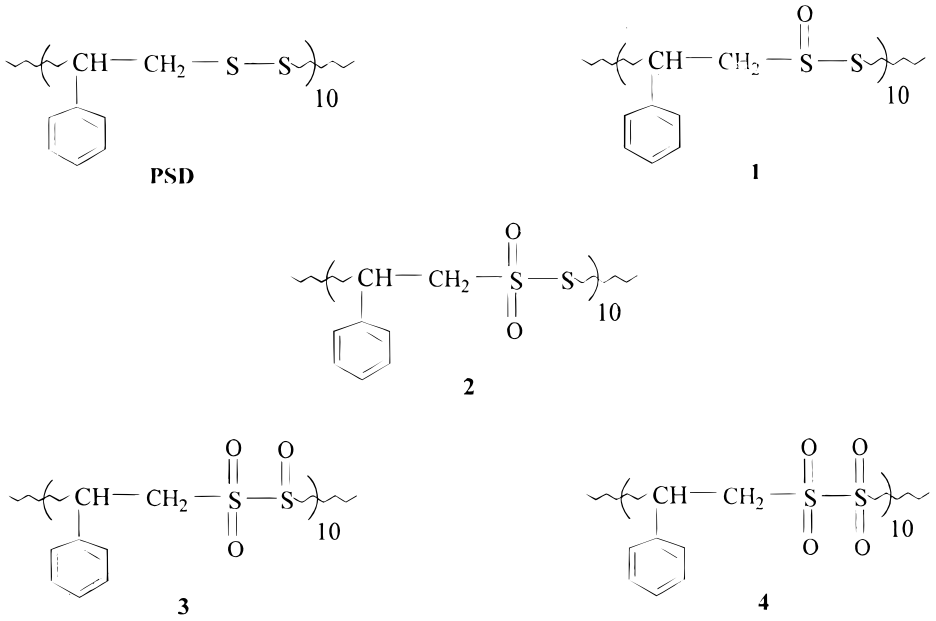

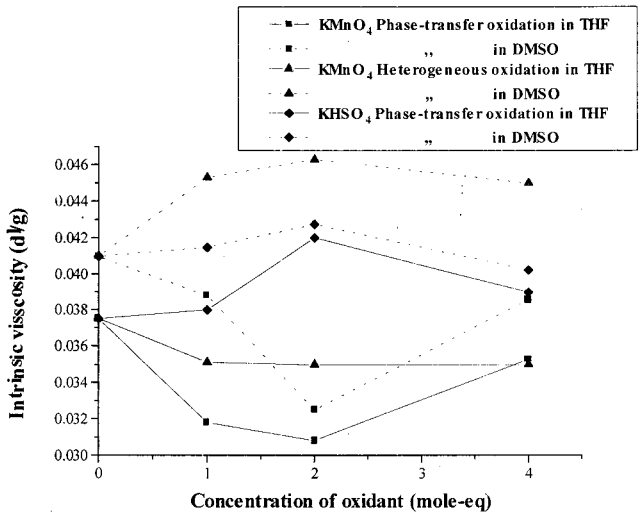

Figure 8. Intrinsic viscosity as a function of oxidant concentration in different solvents. Reaction time: 6 h.

Table 4. T_g of PSD and Oxidized PSD Samples[a]

polymer	T_g (°C)
PSD	4.83
oxidized polymer 1 (OP 1)	63.15
oxidized polymer 2 (OP 2)	64.62
oxidized polymer 3 (OP 3)	63.99

[a]OP 1: $KMnO_4$ heterogeneous oxidized, 4 mol equiv, 6 h, OP 2, OP 3: $KMnO_4$ phase-transfer oxidized, 2 or 4 mol equiv respectively, 6 h.

Since the oxidation of PSD gives a random copolymer encompassing all the possible oxidized structures (Scheme 1), it will be very difficult to individually study each of these oxidized structures experimentally. Hence, information obtained from MD simulation studies will be quite profitable in understanding the behavior of each of the oxidized structures.

We consider here a "single chain dynamics" of an isolated chain of 10 repeat units of PSD as well as its various oxidized counterparts (Scheme 2). In single chain dynamics, the neighboring intermolecular interactions are not considered. In solid or liquid substances, these interactions however will have considerable effect on the shape of the molecule. Although the applicability of the results of a single chain dynamics may be limited in a condensed system, its application for understanding the relative behavior of polymers may be of considerable methodological interest.

The molecular dynamics was carried out using the MSI DISCOVER program. Initially the atoms of the system are assigned Boltzmann distribution at 298 K. Newton's laws of motion are then solved numerically using an integration time step of 1 fs. The relaxation constant for the heat bath variable was fixed at 0.1 ns. A canonical *PVT* ensemble is used with the velocity scaling algorithms to equilibrate the energy of the system so that the potential energy reaches a plateau value. Subsequently, further 1 ns (10^6 time steps) runs were carried out for the data collection.

The MD simulation datas were analyzed to obtain the radius of gyration (R_g) and the trans/gauche ratio. The R_g expression is given as follows:

$$R_g = \left[\frac{1}{n}\sum_{i=1}^{n}(x_1 - x_{cm})^2 + (y_1 - y_{cm})^2 + (z_1 - z_{cm})^2\right]^{1/2}$$

where x_{cm}, y_{cm}, and z_{cm} are the center of mass coordinates and n is the number of atoms. Figure 9 shows the plot of R_g and trans percentage as a function of the number of oxygen atoms per repeat unit of PSD and its oxidized counterparts.

The R_g and trans/gauche ratio both increase with the extent of oxidation but show a decrease from the structure containing three oxygen atoms to the structure containing four oxygen atoms (disulfone) per repeat unit of the chain. The changes in the R_g and trans percentage show an almost similar trend. The initial increase in the R_g is quite consistent with the increase in the trans percentage. It suggests that the chains acquire more and more extended conformation with the extent of oxidation; consequently the R_g values will also increase.

The decrease in the R_g and trans percentage for the disulfone is quite interesting. Being highly electronegative in character, the adjacent S═O groups in disulfone

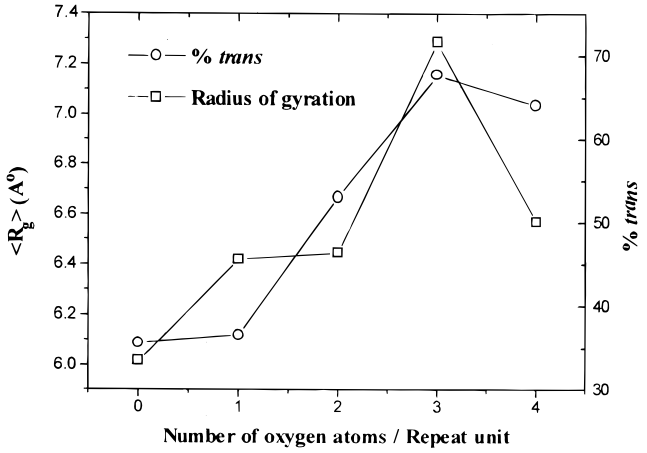

Figure 9. Radius of gyration and trans percentage as a function of number of oxygen atoms in the repeat unit of PSD and its oxidized counterparts.

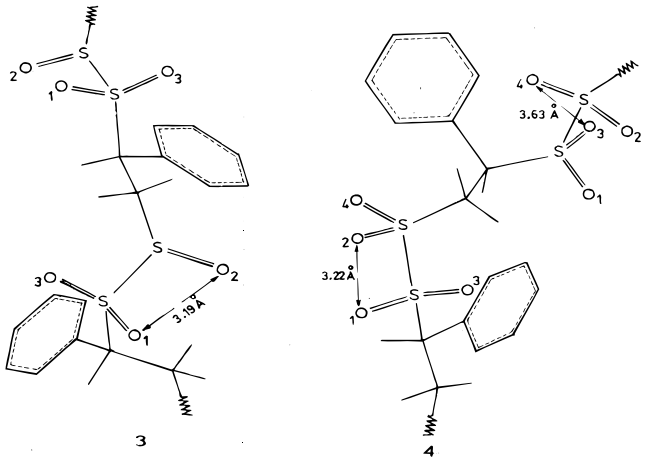

Figure 10. O- - -O distance in partially and fully oxidized PSD (structures **3** and **4**, respectively, in Scheme 2).

Table 5. Comparison of O- - -O Distances in the Oxidized Structures 3 and 4 (Scheme 2)

structure	av dist (Å) O_1- - -O_2	av dist (Å) O_3- - -O_4
3	3.19	
4	3.22	3.63

could be highly unstable, and hence they acquire staggered conformation; as a result the chain would get twisted, thereby decreasing the trans percentage. To confirm this, the O−O distance of adjacent S═O groups were measured for the last two oxidized structures (**3** and **4** in Scheme 2) where reversal in flexibility is observed. The results are given in Table 5 and Figure 10, which clearly shows that the adjacent S═O groups acquire a staggered position in the disulfone structure. Although the oxidation of PSD gives a random copolymer, which encompasses all the oxidized structures, the average R_g of all the oxidized structures is still higher than that of PSD. Even though the R_g and trans percentage for the disulfone structure decreases, it is always higher than that of PSD. Hence, the oxidized sample will always be more rigid than PSD. The rigidity brought about by the extended conformation of the oxidized sample is reflected in their T_g values too, the oxidized polymers have higher T_g compared to PSD (Table 4). Higher [η] observed (Figures 7 and 8) in all the $KHSO_4$-oxidized polymers and in 2−4 mol equiv $KMnO_4$-oxidized PSD is also due to the enhanced rigidity brought about by the SO_2 groups.

Conclusions

The present study has shown that metamorphic oxidation of a disulfide polymer can be brought about by using either a strong oxidizing agent such as $KMnO_4$ or a milder oxidizing agent such as $KHSO_4$. However, $KMnO_4$ also brings about degradation of the polymer chain during oxidation to some extent. It was also found that degradation could be curtailed when the oxidation was done under heterogeneous conditions. The degradation of PSD during oxidation was confirmed by FT−IR, FABMS, and [η] studies. The actual oxidation process was found to be complicated and the product has a random oxidized structure. In fact, FT−IR analysis of all the oxidized polymers shows that both SO and SO_2 groups are present. Increased rigidity of the oxidized polymers is reflected in their T_g. Flexibility of the different oxidized backbones was also examined by molecular dynamics (MD) simulation studies. It was found that the flexibility decreases up to the structure having three oxygen atoms per repeat unit, but thereafter, it increases for the disulfone. However, for the disulfone structure, the increase in flexibility was such that it was still lower than that of the parent disulfide polymer. The reversal in the flexibility was explained on the basis of electrostatic repulsion of adjacent S═O groups in the fully oxidized disulfone structure, which induces a staggered conformation; as a result, its flexibility increases.

The present study has practical relevance because many of these completely oxidized and partially oxidized sulfide polymers could have industrial applications such as compatiblizers and polymeric oxidants etc. Another advantage of the present study is that the polydisulfones, which cannot be synthesized through a direct method, can be prepared by the oxidation of the disulfide polymer itself. As to the complete oxidation of PSD is concerned, it may be pointed out that in the present study we started with a low molecular weight PSD and we did not allow complete oxidation lest the polymer would have degraded significantly. Hence, if the studies are carried out starting with a high molecular weight disulfide polymer, one can make polymers having only disulfone linkages. Also, to get an all polydisulfone structure, further investigations are necessary to find suitable oxidizing agents and conditions for oxidation. But a copolymer having both SO and SO_2 groups can easily be prepared by the present method, and these polymers are expected to have novel properties. Another interesting feature of the present study is that MD simulations could be successfully employed to compare the flexibility of polymer chains.

References and Notes

(1) Fedtke, M. In *Handbook of Polymer Synthesis*; Kricheldorf, H. R., Ed.; Marcel Dekker: New York, 1992; Part B, Chapter 24, p 1503, and references therein.
(2) Elias, H. G. *Macromolecules*; Plenum Press: New York, 1984; Vol. II, Chapter 23, p 801.
(3) Sheng, Q.; Stover, H. D. H. *Macromolecules* **1997**, *30*, 6451.
(4) Hirao, A.; Shione, H.; Ishizone, T.; Nakahama, S. *Macromolecules* **1997**, *30*, 3728.

(5) Spassky, N.; Sepulchre, M.; Sigwalt, P. In *Handbook of Polymer Synthesis*; Kricheldorf, H. R., Ed.; Marcel Dekker: New York, 1992; Part B, Chapter 16, p 1037, and references therein.
(6) Durst, T. In *Comprehensive Organic Chemistry*; Jones, N., Ed.; Pergamon Press: Oxford, England, 1979; Vol. 3, Part 11.9, and references therein.
(7) Uemura, S. In *Comprehensive Organic Synthesis*; Trost, B. M., Ed.; Pergamon Press: Oxford, England, 1991; Vol. 7; Chapter 6.2, p 757, and references therein.
(8) Fawcett, A. H. In *Encyclopedia of Polymer Science and Engineering*; Mark, H. F., Bikales, N. M., Overberger, C. G., Menges, G., Eds.; Wiley: New York, 1987; Vol. 10, p 408, and references therein.
(9) Lee, J. C.; Litt, M. H.; Rogers, C. E. *Macromolecules* **1997**, *30*, 3766.
(10) Oyama, T.; Ozaki, J.; Chujo, Y. *Polym. Bull.* **1997**, *38*, 379.
(11) Zhang, T.; Litt, M. H.; Rogers, C. E. *J. Polym. Sci., Part. A: Polym. Chem.* **1994**, *32*, 1323.
(12) Orgeret- Ravanat, C.; Galin, J.-C. *Makromol. Chem.* **1988**, *189*, 2017.
(13) Macro, C.; Fatou, J. G.; Bello, A.; Perena, J. M. *Makromol. Chem.* **1984**, *185*, 1255 and references therein.
(14) Macro, C.; Bello, A.; Perena, J. M.; Fatou, J. G. *Macromolecules* **1983**, *16*, 95.
(15) Price, C. C.; Blair, E. A. *J. Polym. Sci., Part A-1* **1967**, *5*, 171.
(16) Noshay, A.; Price, C. C. *J. Polym. Sci.* **1961**, *54*, 533.
(17) Marvel, C. S.; Weil, E. D. *J. Am. Chem. Soc.* **1954**, *76*, 61.
(18) Carothers, W. H. U.S. pat. 2,201,884, 1940; *Chem. Abstr.* **1940**, *34*, 6389.
(19) Kishore, K.; Ganesh, K. *Adv. Polym. Sci.* **1995**, *121*, 81.
(20) Murthy, K. S.; Ganesh, K.; Kishore, K. *Polymer* **1996**, *37*, 5541.
(21) Ganesh, K.; Latha, R.; Kishore, K.; Ninan, K. N.; George, B. *J. Appl. Polym. Sci.* **1997**, *66*, 2149.
(22) Ganesh, K.; Kishore, K. *Macromolecules* **1995**, *28*, 2483.
(23) Ganesh, K.; Latha, R.; Kishore, K. *Macromolecules* **1996**, *29*, 5231.
(24) Kishore, K.; Ganesh, K. *Macromolecules* **1993**, *26*, 4700.
(25) Foti, S.; Montaudo, G. In *Analysis of Polymer Systems*; Bark, L. S.; Allen, N. S., Eds.; Applied Science: London, 1982; 103.
(26) Montaudo, G.; Puglisi, C. In *Comprehensive Polymer Science*; Aggarwal, S., Russo, S., Eds.; Pergamon: Oxford, England, 1992; 1st Suppl., p 227, and references therein.
(27) Montaudo, G.; Puglisi, C.; de Leeuw, J. W.; Hartgers, W.; Kishore, K.; Ganesh, K. *Macromolecules* **1996**, *29*, 6466.
(28) Montaudo, G.; Puglisi, C.; Blazso, M.; Kishore, K.; Ganesh, K. *J. Anal. Appl. Pyrol.* **1994**, *29*, 207.
(29) Noureldin, N. A.; McConnell, W. B.; Lee, D. G. *Can. J. Chem.* **1984**, *62*, 2113.
(30) Rieke, R. D.; Rhyne, L. D. *J. Org. Chem.* **1979**, *44*, 3446.
(31) Block, E.; DeOrazio, R.; Mohan, T. *J. Org. Chem.* **1994**, *59*, 2273.
(32) Madesclaire, M. *Tetrahedron* **1986**, *42*, 5459.
(33) Wolfe, S.; Ingold, C. F. *J. Am. Chem. Soc.* **1983**, *105*, 7755.
(34) Schueddemage, H. D. R.; Hummel, D. O. *Adv. Mass Spectrom.* **1968**, *4*, 857.
(35) Davies, J. D.; Daly, W. H. *Polym. Prepr. (Am. Chem. Soc., Div. Polym. Chem.)* **1997**, *38* (1), 745.

MA981715D